



HAL
open science

A nonlinear Schrödinger equation for capillary waves on arbitrary depth with constant vorticity

Christian Kharif, Malek Abid, Yang-Yih Chen, Hung-Chu Hsu

► **To cite this version:**

Christian Kharif, Malek Abid, Yang-Yih Chen, Hung-Chu Hsu. A nonlinear Schrödinger equation for capillary waves on arbitrary depth with constant vorticity. 2024. hal-04535263

HAL Id: hal-04535263

<https://cnrs.hal.science/hal-04535263>

Preprint submitted on 6 Apr 2024

HAL is a multi-disciplinary open access archive for the deposit and dissemination of scientific research documents, whether they are published or not. The documents may come from teaching and research institutions in France or abroad, or from public or private research centers.

L'archive ouverte pluridisciplinaire **HAL**, est destinée au dépôt et à la diffusion de documents scientifiques de niveau recherche, publiés ou non, émanant des établissements d'enseignement et de recherche français ou étrangers, des laboratoires publics ou privés.

Banner appropriate to article type will appear here in typeset article

A nonlinear Schrödinger equation for capillary waves on arbitrary depth with constant vorticity

Christian Kharif¹, Malek Abid¹, Yang-Yih Chen² and Hung-Chu Hsu² †

¹Aix-Marseille Université, Institut de Recherche sur les Phénomènes Hors Equilibre, UMR 7342, CNRS, Centrale Méditerranée, Marseille, 13384, France

²Department of Marine Environment and Engineering, National Sun Yat-Sen University, Kaohsiung 80424, Taiwan

(Received xx; revised xx; accepted xx)

A nonlinear Schrödinger equation for pure capillary waves propagating at the free surface of a vertically sheared current has been derived to study the stability and bifurcation of capillary Stokes waves on arbitrary depth.

A linear stability analysis of weakly nonlinear capillary Stokes waves on arbitrary depth has shown that (i) the growth rate of modulational instability increases as the vorticity decreases whatever the dispersive parameter kh where k is the carrier wavenumber and h the depth (ii) the growth rate is significantly amplified for shallow water depths and (iii) the instability bandwidth widens as the vorticity decreases. A particular attention has been paid to damping due to viscosity and forcing effects on modulational instability. In addition, a linear stability analysis to transverse perturbations in deep water has been carried out, demonstrating that the dominant modulational instability is two-dimensional whatever the vorticity.

Near the minimum of linear phase velocity in deep water, we have shown that generalized capillary solitary waves bifurcate from linear capillary Stokes waves when the vorticity is positive.

Moreover, we have shown that the envelope of pure capillary waves in deep water is unstable to transverse perturbations. Consequently, deep water generalized capillary solitary waves are expected to be unstable to transverse perturbations.

1. Introduction

The effect of wind blowing above the air-sea interface is twofold: (i) it generates short waves that take place within the first millimeters to meters, and (ii) it generates a shear flow in the uppermost layer of the water. Consequently, these waves propagate in the presence of vorticity. These small scales participate in the exchanges of momentum, energy and mass across the air-sea interface. An accurate description of the surface stress is important in modelling and forecasting ocean wave dynamics. In addition, the knowledge of their properties is crucial for satellite remote sensing applications.

In this paper, we focus our study on weakly nonlinear capillary waves propagating at the free surface of a flow of constant vorticity. One of our aims is to complete and extend to finite depth the preliminary results of Hsu *et al.* (2018) and Dhar & Kirby (2023) on pure capillary

† Email address for correspondence: christian.kharif@centrale-med.fr

37 waves on deep water in the presence of constant vorticity. Hsu *et al.* (2018) used the cubic
38 nonlinear Schrödinger equation, whereas Dhar & Kirby (2023) used a fourth-order nonlinear
39 Schrödinger equation. Hsu *et al.* (2018) investigated the effect of a shear current of constant
40 vorticity on the modulational instability of weakly nonlinear periodic gravity-capillary wave
41 trains. To do this, they derived a cubic nonlinear Schrödinger equation for gravity-capillary
42 water waves on arbitrary depth with constant vorticity. To extend their results in the absence of
43 acceleration due to gravity, we consider the nonlinear Schrödinger equation for pure capillary
44 water waves on finite-depth currents of constant vorticity. Later on, within the framework a
45 fourth-order nonlinear Schrödinger equation Dhar & Kirby (2023) investigated the stability
46 of periodic gravity-capillary waves on arbitrary depth in the presence of constant vorticity.
47 To the best of our knowledge, there is no study on the stability of pure capillary waves on
48 finite depth in the presence of constant vorticity.

49 On the other hand, several studies have been devoted to the stability of steadily propagating
50 periodic capillary waves on deep water, but without vorticity. Chen & Saffman (1985)
51 investigated the three-dimensional stability and bifurcation of capillary waves and gravity
52 waves on deep water. To do this, they used the approach detailed by McLean (1982) for the
53 fully nonlinear waves and the nonlinear Schrödinger equation for the modulational instability
54 of weakly nonlinear capillary waves. Hogan (1985) derived from the Zakharov equation a
55 fourth-order nonlinear Schrödinger equation in deep water and found that the mean flow
56 effect on weakly nonlinear pure capillary waves are of opposite sign to those of pure gravity
57 waves. Zhang & Melville (1986) considered the stability of weakly nonlinear gravity-capillary
58 waves on deep water in the range of capillary waves of few millimeters. They focused their
59 study on triad and quartet instabilities. Hogan (1988) found two superharmonic bubbles of
60 instability of the exact nonlinear capillary wave solutions of Crapper (1957) at amplitudes
61 less than the maximum. Tiron & Choi (2012) investigated the stability of the exact deep
62 water capillary waves (Crapper's solutions). They found that Crappers's capillary waves are
63 stable to superharmonic disturbances whatever the amplitude and unstable to subharmonic
64 disturbances. Later on, Murashige & Choi (2020) considered the stability of Crapper's
65 capillary waves on deep water to weakly three-dimensional disturbances. They found that
66 Crapper's solutions are stable to two-dimensional superharmonic disturbances and unstable
67 to three-dimensional superharmonic disturbances.

68 In the absence of vorticity, the existence of solitary gravity-capillary waves on deep water
69 was proved numerically by Longuet-Higgins (1989). Later on, Akylas (1993), using the
70 nonlinear Schrödinger equation in deep water, showed that gravity-capillary solitary waves
71 occur when the phase velocity of the carrier wave matches the group velocity of the envelope
72 soliton solution. The linear dispersion relation of gravity-capillary waves has a minimum
73 in phase velocity, which is equal to the group velocity. Consequently, for values less than
74 this extremum two-dimensional gravity-capillary waves may bifurcate into solitary waves
75 in deep water. Abid *et al.* (2019) found that gravity-capillary solitary waves with decaying
76 oscillatory tails exist in deep water in the presence of constant vorticity. For a review on this
77 problem, one can refer to Dias & Kharif (1999). Steady three-dimensional gravity-capillary
78 waves were investigated by Kim & Akylas (2005), Milewski (2005) and Părău *et al.* (2005).
79 To the best of our knowledge, this bifurcation phenomenon has not been considered for pure
80 capillary waves. This can be easily understood, since the linear dispersion relation of pure
81 capillary waves has no minimum in phase velocity in the absence of vorticity.

82 In section 2 the nonlinear Schrödinger equation for capillary waves is given, and the physical
83 phenomena associated with the singularities of the nonlinear coefficient are discussed.
84 Section 3 is devoted to the stability analysis of periodic capillary waves on arbitrary depth
85 in the presence of constant vorticity. Bifurcation of generalized solitary waves on deep
86 water from periodic capillary wave trains is considered in section 4. Transverse instability of

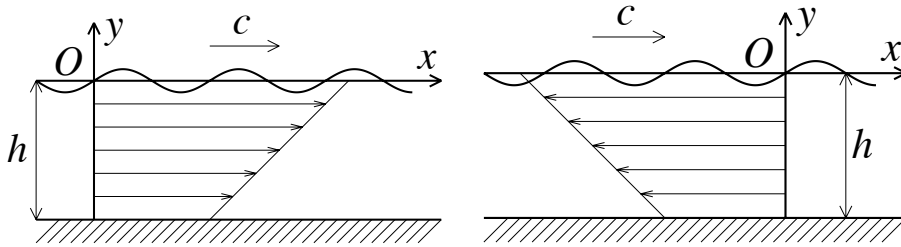


Figure 1: Sketches of waves on a shear current in the fixed reference frame. Downstream propagation (left). Upstream propagating (right).

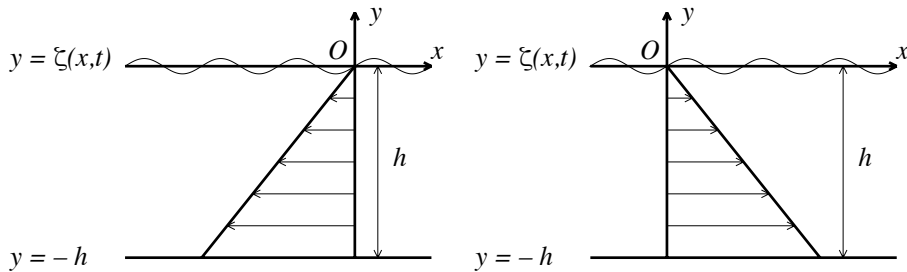


Figure 2: Sketches of waves on a shear current in the moving reference frame. Downstream propagation (left). Upstream propagating (right).

87 capillary envelope soliton and uniform capillary wave trains in deep water is considered in
88 section 5.

89 2. Nonlinear Schrödinger equation for pure capillary waves

90 The unperturbed flow is a weakly nonlinear capillary wave train traveling steadily at the
91 free surface of a vertically sheared current of constant vorticity (see figure 1). The fluid is
92 assumed incompressible and inviscid.

93 In the fixed frame, the underlying current velocity is $u_0(y) = U_0 + \Omega y$, where Ω is the shear
94 (the current intensity) and U_0 the current velocity at the free surface $y = 0$. The waves are
95 stationary on a stream. Note that the vorticity is $-\Omega$. Downstream propagation corresponds
96 to negative vorticity, whereas upstream propagation corresponds to positive vorticity.
97 Being primarily interested in the effect of the vorticity, we choose a reference frame moving
98 with U_0 (see figure 2). In the moving frame, the fluid velocity is

$$99 \quad \mathbf{u}(x, y) = (\Omega y + \phi_x, \phi_y).$$

100 where (ϕ_x, ϕ_y) is the wave induced velocity.

101 The waves are potential due to the Kelvin theorem, which states that vorticity is conserved
102 for a two-dimensional flow of an incompressible and inviscid fluid with external forces derived
103 from a potential. There is no loss of generality if the study is restricted to carrier waves with
104 positive phase speeds, so long as both positive and negative values of Ω are considered.

105 The governing equations are the Laplace equation (equation (2.1)) with the kinematic and
106 dynamic boundary conditions (equations (2.2)-(2.3)) and the bottom condition (equation
107 (2.4)).

$$108 \quad \Delta\phi(x, y, t) = 0, \quad -h < y < \zeta(x, t), \quad (2.1)$$

109 where $\zeta(x, t)$ is the surface elevation.

$$110 \quad \zeta_t + \zeta_x(\phi_x + \Omega y) - \phi_y = 0, \quad y = \zeta(x, t). \quad (2.2)$$

$$112 \quad \phi_t + \frac{1}{2}(\nabla\phi)^2 + \Omega\zeta\phi_x - \Omega\psi - \frac{T}{\rho_w} \frac{\zeta_{xx}}{(1 + \zeta_x^2)^{3/2}} = 0, \quad y = \zeta(x, t), \quad (2.3)$$

113 where ψ is the stream function, T the surface tension and ρ_w the water density.

114 Without loss of generality, the atmospheric pressure, P_a , is set equal to zero.

$$115 \quad \phi_y = 0, \quad y = -h. \quad (2.4)$$

116 Following Thomas *et al.* (2012) and Hsu *et al.* (2018), the stream function ψ can be removed

117 by differentiating equation (2.3) with respect to x and using the Cauchy-Riemann relations.

118 The dynamic boundary condition becomes for weakly nonlinear water waves

$$119 \quad \begin{aligned} & \phi_{tx} + \phi_{ty}\zeta_x + \phi_x(\phi_{xx} + \phi_{xy}\zeta_x) + \phi_y(\phi_{xy} + \phi_{yy}\zeta_x) + \Omega\zeta_x\phi_x \\ & + \Omega\zeta(\phi_{xx} + \phi_{xy}\zeta_x) + \Omega(\phi_y - \phi_x\zeta_x) \\ & - \frac{T}{\rho_w}(\zeta_{xxx} - \frac{3}{2}\zeta_x^2\zeta_{xxx} - 3\zeta_{xx}^2\zeta_x) = 0, \quad y = \zeta(x, t), \end{aligned} \quad (2.5)$$

123 that corresponds to that of Hsu *et al.* (2018) for $g = 0$.

124 The method of multiple scales is used to derive the spatio-temporal evolution of the complex

125 envelope, $a(\xi, \tau)$, of the free surface elevation $\zeta(x, t)$.

$$126 \quad \zeta(x, t) = \frac{1}{2} \{ \epsilon a(\xi, \tau) \exp(i(kx - \omega t)) + c.c. \} + \mathcal{O}(\epsilon^2),$$

127 where $\xi = \epsilon(x - c_g t)$, $\tau = \epsilon^2 t$, c_g , k and ω are the group velocity, wavenumber and frequency

128 of the carrier wave and ϵ a small parameter.

129 The nonlinear Schrödinger equation governing the evolution of the complex envelope of a

130 packet of capillary waves on finite depth in the presence of constant vorticity (vor-NLS) is

$$131 \quad ia_\tau + La_\xi\xi + N|a|^2a = 0. \quad (2.6)$$

132 where the dispersive coefficient L and nonlinear coefficient N are

$$133 \quad L = \frac{\omega}{k^2(2+X)^3\sigma^2} \left[3(1+X)(1+X+X^2)\sigma^2 - 6(1+X)^2\mu\sigma(\sigma^2-1) + \right. \\ \left. \mu^2(\sigma^2-1)\left((1+X)^2 + (3+2X)\sigma^2\right) \right] \quad (2.7)$$

136 and

$$137 \quad N = -\frac{\omega k^2}{8\sigma^2} \left[\sigma^2 \frac{5+3X}{2+X} - \frac{P_0 + P_1X + P_2X^2 + P_3X^3 + X^4}{(3-\sigma^2+3X)(2+X)} \right. \\ \left. + 2\sigma(2+X) \left(\frac{(1+X)^2 - \sigma^2}{(1-\sigma^2)\mu + 3\sigma(1+X)} + \frac{1-\sigma^2}{\mu((1-\sigma^2)+X(2+X)) + 3\sigma(1+X)} \right) \right], \quad (2.8)$$

141 with $\mu = kh$, $\sigma = \tanh \mu$, $X = \sigma\Omega/\omega$ and $P_0 = 21 - 10\sigma^2 + \sigma^4$, $P_1 = 42 + 2\sigma^2 - 4\sigma^4$,

142 $P_2 = 30 + 12\sigma^2$, $P_3 = 9 + 5\sigma^2$.

143 Note that $|X|$ can be considered as a Strouhal number, which is the ratio between the

144 characteristic frequency of the vorticity and that of the capillary waves.

145 The coefficients L and N given by equations (2.7) and (2.8) correspond to those of Hsu *et al.*
 146 (2018) for $\kappa = k^2 T / (\rho_w g) \rightarrow \infty$ and $\Omega \neq 0$ and to those of Djordjevic & Redekopp (1977)
 147 in finite depth for $\kappa \rightarrow \infty$ and $\Omega = 0$.

148 The linear dispersion relation of capillary waves in the presence of constant vorticity is

$$149 \quad \omega^2 + \sigma \Omega \omega - \sigma \frac{k^3 T}{\rho_w} = 0. \quad (2.9)$$

150 From (2.9) it is easy to show that $X > -1$.

151 As emphasized above, we consider a carrier wave propagating from left to right of frequency
 152 ω , phase velocity c_p and group velocity c_g whose expressions are

$$153 \quad \omega = -\frac{\sigma \Omega}{2} + \sqrt{\left(\frac{\sigma \Omega}{2}\right)^2 + \sigma \frac{k^3 T}{\rho_w}}, \quad (2.10)$$

154

$$155 \quad c_p = -\frac{\sigma \Omega}{2k} + \sqrt{\left(\frac{\sigma \Omega}{2k}\right)^2 + \sigma \frac{kT}{\rho_w}}, \quad (2.11)$$

156

$$157 \quad c_g = -\frac{\Omega h}{2}(1 - \sigma^2) + \frac{(1 - \sigma^2)(\Omega^2 h \sigma / 2 + \mu k^2 T / \rho_w) + 3\sigma k^2 T / \rho_w}{\sqrt{(\Omega \sigma)^2 + 4\sigma k^3 T / \rho_w}}. \quad (2.12)$$

158 The nonlinear coefficient N presents two singularities that one should avoid, either

$$159 \quad 3 - \sigma^2 + 3X = 0, \quad (2.13)$$

160 or

$$161 \quad \mu((1 - \sigma^2) + X(2 + X)) + 3\sigma(1 + X) = 0. \quad (2.14)$$

162

163 Equation (2.13) corresponds to the reduction of the second-harmonic resonance condition of
 164 gravity-capillary waves propagating at the free surface of an underlying current of constant
 165 vorticity when g goes to zero (κ goes to ∞). This resonance which is also called the Wilton
 166 ripple phenomenon was investigated by Martin & Matioc (2013) who proved rigorously the
 167 existence of Wilton ripples on finite depth for water waves with constant positive vorticity
 168 and capillary effect. However, their study focused on integer values of the wavenumber.
 169 The Wilton ripple phenomenon occurs when both the fundamental mode and the second
 170 harmonic have the same phase velocity, that is, when the phase velocity presents a minimum
 171 value. Note that in the absence of positive vorticity ($\Omega < 0$) there is no minimum of phase
 172 velocity for pure capillary waves. The phase velocity c_p reaches a minimal value when $\Omega < 0$
 173 (positive vorticity) and $k = k_m$ given in deep water by

$$174 \quad k_m = \left(\frac{2\rho_w}{T}\Omega^2\right)^{1/3}. \quad (2.15)$$

175 The wavenumber k satisfying $c_p(k) = c_p(2k)$ is

$$176 \quad k = \left(\frac{3\rho_w}{4T}\Omega^2\right)^{1/3}. \quad (2.16)$$

177 The second-harmonic resonance corresponds to the following degenerate resonant triad

$$178 \quad 2k_1 - k_2 = 0,$$

$$179 \quad 2\omega_1 - \omega_2 = 0,$$

180 where

$$181 \quad \omega_1 = -\frac{\Omega}{2} + \sqrt{\left(\frac{\Omega}{2}\right)^2 + \frac{T}{\rho_w} k^3}, \quad (2.17)$$

182

$$183 \quad \omega_2 = -\frac{\Omega}{2} + \sqrt{\left(\frac{\Omega}{2}\right)^2 + \frac{8T}{\rho_w} k^3}, \quad (2.18)$$

184 with k given by (2.16).

185 Injecting the expression of k in (2.17) and (2.18), we obtain $\omega_1 = -3\Omega/2$ and $\omega_2 = -3\Omega$.

186 Constantin & Kartashova (2009) showed that only positive vorticity ($\Omega < 0$) can trigger the
187 occurrence of three-wave resonant interactions of capillary water waves on an underlying
188 current of constant vorticity. As Martin & Matic (2013) they considered integer values of
189 the wavenumber.

190 We have shown that the Wilton ripple phenomenon exists in infinite depth for pure capillary
191 waves travelling on a current of constant positive vorticity. To a given fixed value of the
192 vorticity, $-\Omega$, corresponds a resonant real-valued wavenumber given by (2.16) and inversely,
193 to a given fixed real-valued resonant wavenumber, k , corresponds a value of the shear
194 $\Omega = -\sqrt{4Tk^3}/(3\rho_w)$. Fixing $k = 1$ gives the minimal value of the vorticity found by
195 Constantin & Kartashova (2009). Note that within the framework of capillary water waves,
196 the vorticity must be strong to trigger the second-harmonic resonance.

197 The wavenumber given by equation (2.16) does not satisfy equation (2.13) unless $\sigma = 1$
198 that does not mean that there are no second-harmonic resonances in finite depth within the
199 framework of pure capillary waves.

200 The second singularity corresponds to the reduction of the short wave/long wave resonance of
201 gravity-capillary propagating at the free surface of an underlying current of constant vorticity
202 when g goes to zero. Note that this singularity disappears in the nonlinear coefficient N when
203 $\sigma = 1$, that is, in deep water. Nevertheless, this does not mean that there are no resonant triad
204 interactions in deep water.

205 Equation (2.14) has two real-valued negative roots: one is less than minus one and is ruled
206 out because $X > -1$ and the other belongs to $(-1, 0)$ when μ ranges from zero to infinity. It
207 is useful to note that whatever the depth, there exists a singular value of X for $-1 < X < 0$.
208 Constantin & Kartashova (2009) demonstrated that in deep water, capillary waves on a
209 current of positive vorticity ($\Omega < 0$) may give rise to resonant triads.

210 We found in finite depth triads of capillary waves satisfying the following resonance
211 conditions

$$212 \quad k_1 - k_2 + k_3 = 0,$$

$$214 \quad \omega_1 - \omega_2 + \omega_3 = 0,$$

215 with

$$216 \quad \omega_i = -\frac{\sigma\Omega}{2} + \sqrt{\left(\frac{\sigma\Omega}{2}\right)^2 + \sigma \frac{k_i^3 T}{\rho_w}}, \quad i = 1, 2, 3. \quad (2.19)$$

217 To illustrate this feature of capillary waves on a current of constant positive vorticity in
218 finite depth, three examples are shown in figure 3 which gives pairs of capillary waves
219 of wavenumbers (k_1, k_2) that excite a third wave of wavenumber k_3 . To a given value of
220 k_1 corresponds a value of k_2 and consequently a value of k_3 . The three curves present a
221 minimum for the wavenumber k_2 .

222 We can conclude that (2.14) corresponds to resonant triads of capillary waves in finite depth

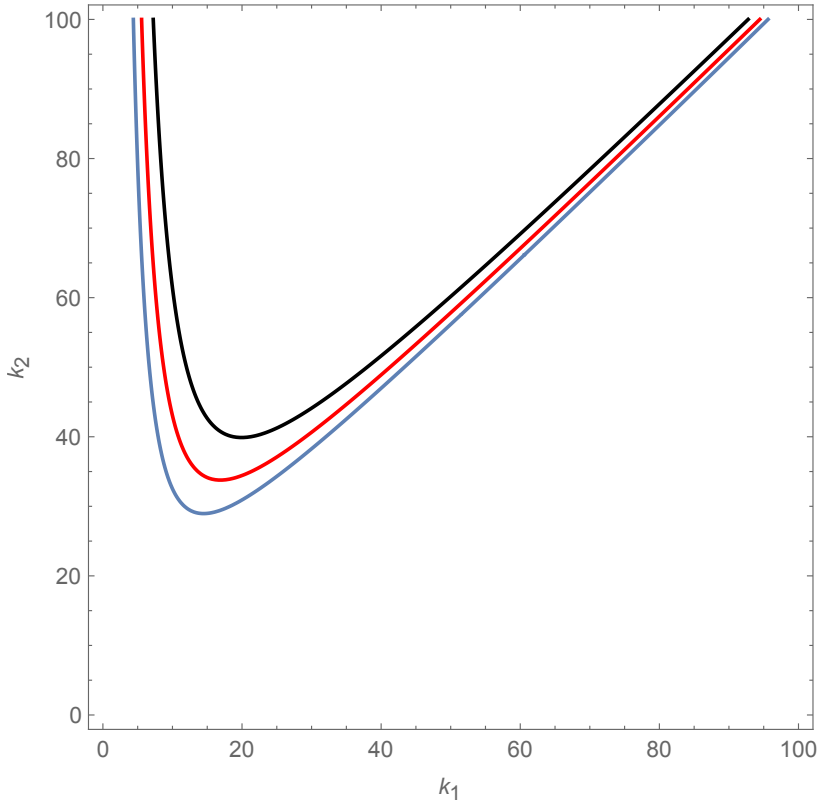


Figure 3: Resonant triad in finite depth: a pair of wavenumbers (k_1, k_2) exciting a third wavenumber $k_3 = k_2 - k_1$. $\mu = 1$ (black solid line), $\mu = 0.5$ (red solid line), $\mu = 0.3$ (blue solid line)

223 with positive constant vorticity. At any depth, there exists a forbidden positive vorticity value
 224 corresponding to a resonant triad.

225 3. Stability of weakly nonlinear capillary waves on arbitrary depth with constant 226 vorticity

227 The NLS equation (2.6) admits the Stokes' wave solution

$$228 \quad a = a_0 \exp(iNa_0^2\tau), \quad (3.1)$$

229 with the initial condition a_0 .

230 Let us consider an infinitesimal disturbance of this solution so that the perturbed solution is
 231 written as follows

$$232 \quad a' = a_0(1 + \delta_a) \exp(iNa_0^2\tau) \exp(i\delta_w). \quad (3.2)$$

233 Substituting the expression (3.2) of the perturbed solution in the NLS equation (2.6),
 234 linearizing and separating between real and imaginary parts leads to a system of linear
 235 coupled partial differential equations with constant coefficients. Consequently, this system
 236 admits solutions of the following forms,

$$237 \quad \delta_a = (\delta_a)_0 \exp(i(p\xi - \Gamma\tau)),$$

238

239

$$\delta_w = (\delta_w)_0 \exp(i(p\xi - \Gamma\tau)),$$

240 where the real p is the perturbation wavenumber.

241 The necessary and sufficient condition for the existence of a non-trivial solution is

242

$$\Gamma^2 = p^2(L^2p^2 - 2NLa_0^2).$$

243 The Stokes' wave solution is stable when $L^2p^2 - 2NLa_0^2 \geq 0$ and unstable when $L^2p^2 -$
244 $2NLa_0^2 < 0$.

245 The growth rate of instability is

246

$$\Gamma_i = p(2NLa_0^2 - L^2p^2)^{1/2}. \quad (3.3)$$

247 The maximal growth rate of instability is

248

$$\Gamma_{imax} = \sqrt{\frac{N}{L}} \sqrt{NLa_0^2}, \quad (3.4)$$

249 for $p = \sqrt{\frac{N}{L}} a_0$.250 Note that instability occurs when $LN > 0$.251 For $\Omega = 0$ the rate of growth of the modulational instability of pure capillary waves on finite
252 depth is,

253

$$\Gamma_i = \frac{\omega}{8k^2} \sqrt{3a_0^2k^4p^2 - 9p^4}.$$

254 which can be found in Hsu *et al.* (2018) and Chen & Saffman (1985). The maximum growth
255 rate is $\omega(a_0k)^2/16$, corresponding to the wavenumber $p_{\max} = a_0k^2/\sqrt{6}$.256 We introduce dimensionless coefficients $\tilde{L} = k^2L/\omega$ and $\tilde{N} = N/(\omega k^2)$ so that the dispersive
257 and nonlinear coefficients of the NLS equation are functions of $\mu = kh$ and $X = \sigma\Omega/\omega$.

258 The dimensionless growth rate of instability reads

259

$$\frac{\Gamma_i}{\omega(a_0k)^2} = \tilde{p}(2\tilde{N}\tilde{L} - \tilde{L}^2\tilde{p}^2)^{1/2}, \quad (3.5)$$

260 with $\tilde{p} = p/(a_0k^2)$ and its maximal value is

261

$$\frac{\Gamma_{imax}}{\omega(a_0k)^2} = \sqrt{\frac{\tilde{N}}{\tilde{L}}} \sqrt{\tilde{N}\tilde{L}}, \quad (3.6)$$

262 for $\tilde{p} = \sqrt{\tilde{N}/\tilde{L}}$.

263 The dimensionless bandwidth of instability is

264

$$\Delta\tilde{p} = \sqrt{2\frac{\tilde{N}}{\tilde{L}}}, \quad \frac{\Delta p}{k} = \Delta\tilde{p} a_0k. \quad (3.7)$$

265 The analytic expression of the dimensionless maximal growth rate of instability in deep water
266 reads

267

$$\frac{\Gamma_{imax}}{\omega(a_0k)^2} = \frac{3 + 14X + 23X^2 + 11X^3 - 3X^4}{24(X+1)(3X+2)}. \quad (3.8)$$

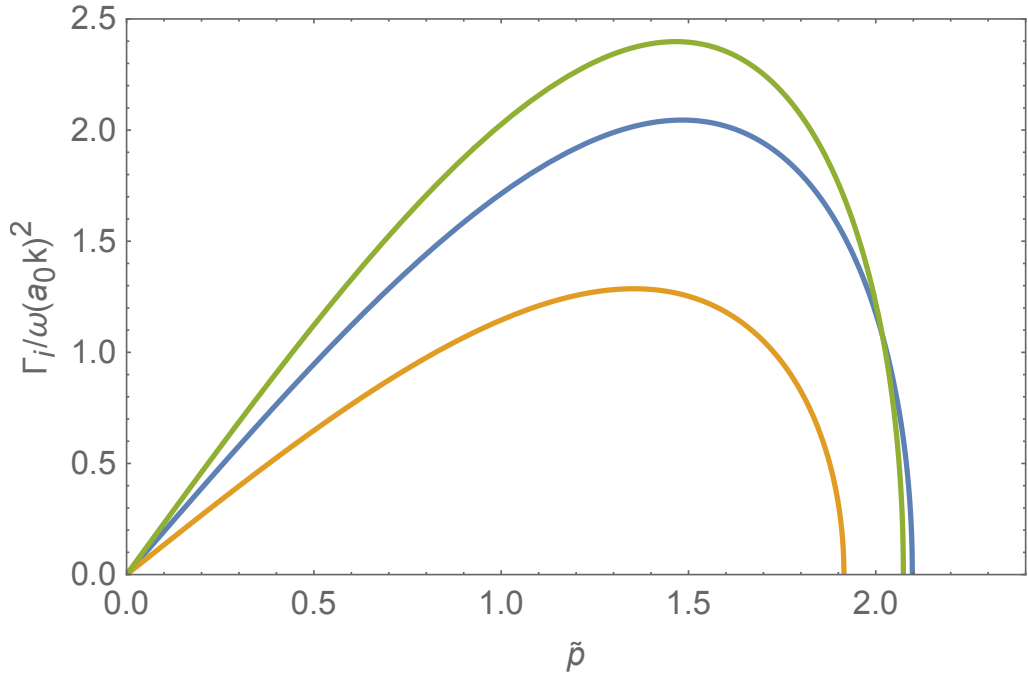


Figure 4: Dimensionless growth rate of instability as a function of the dimensionless perturbation wavenumber for $kh = 0.30$ and $X = -0.40$ (orange solid line), $X = 0$ (blue solid line), $X = 0.40$ (green solid line).

268 For weak vorticity equation (3.8) becomes

$$269 \quad \frac{\Gamma_{imax}}{\omega(a_0 k)^2} = \frac{1}{16} \left(1 + \frac{13}{6} X + \frac{3}{4} X^2 \right) + \mathcal{O}(X^3).$$

270 On figures 4- 7 is plotted the dimensionless growth rate of instability given by (3.5) as a
 271 function of the dimensionless perturbation wavenumber \tilde{p} for several values of the depth
 272 and vorticity. The dimensionless growth rate of instability increases as the dimensionless
 273 shear increases and as the dimensionless vorticity decreases for a given value of the depth.
 274 This feature can be observed whatever the depth. For negative dimensionless vorticity the
 275 dimensionless growth rate of instability increases as the depth decreases. This feature is still
 276 present in shallow water for positive vorticity. The bandwidth of instability increases as the
 277 depth decreases.

278 Figure 8 shows the dimensionless maximal growth rate of instability as a function of the
 279 dimensionless depth, $\mu = kh$ for several values of the dimensionless vorticity. We observe that
 280 it starts to increase significantly while $\mu < 2$. In finite and infinite depths, positive (negative)
 281 dimensionless vorticity increases (reduces) the dimensionless growth rate of instability. In
 282 shallow water, this feature persists only for weak dimensionless vorticity.

283 In figure 9 is plotted the dimensionless maximal growth rate of instability as a function of the
 284 vorticity for several values of the dimensionless depth. For about $X < 3$ the dimensionless
 285 maximal growth rate of instability increases as the depth decreases, whereas for about $X > 3$
 286 it increases as the depth increases.

287 Within the framework of irrotational flow ($X = 0$), Tiron & Choi (2012) investigated
 288 the stability of the exact deep water capillary wave solution, derived by Crapper (1957), to
 289 two-dimensional infinitesimal disturbances. In figure 10 is plotted the dimensionless growth

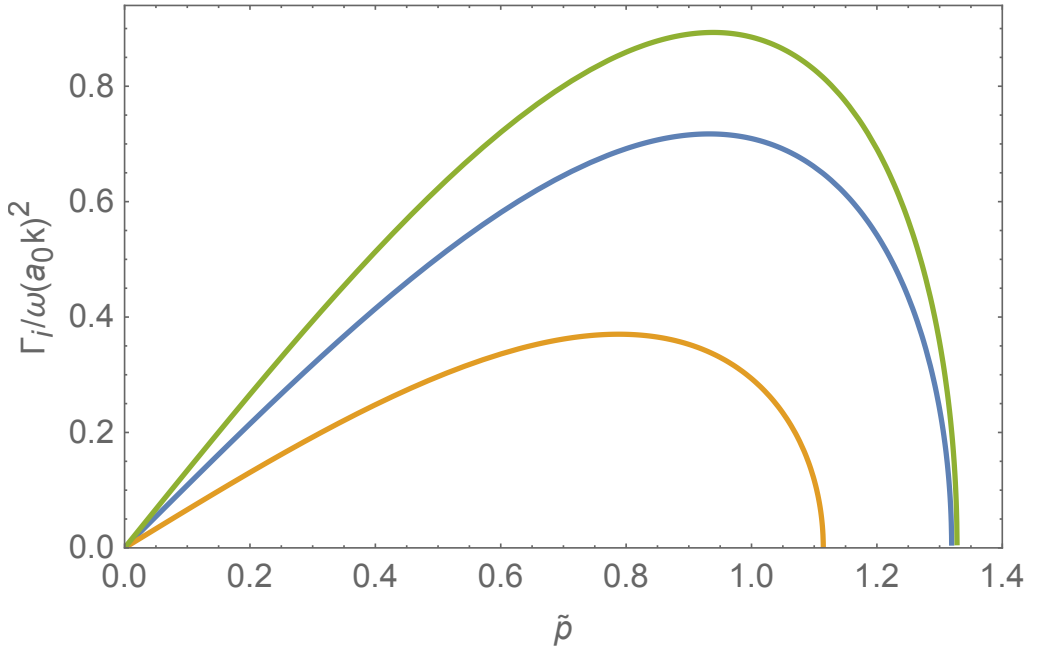


Figure 5: Dimensionless growth rate of instability as a function of the dimensionless perturbation wavenumber for $kh = 0.50$ and $X = -0.40$ (orange solid line), $X = 0$ (blue solid line), $X = 0.40$ (green solid line).

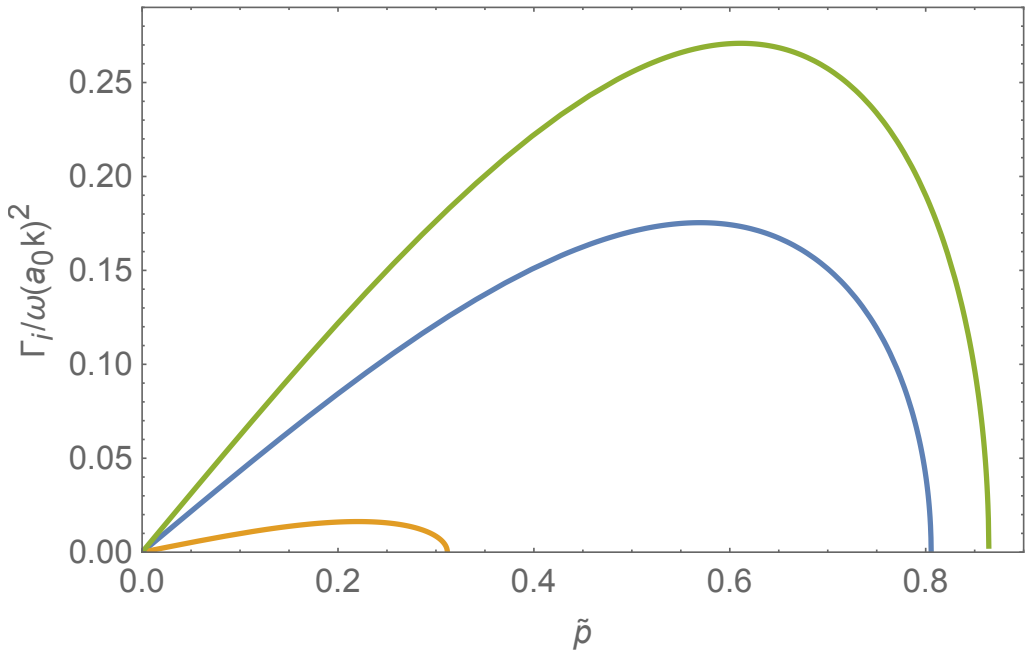


Figure 6: Dimensionless growth rate of instability as a function of the dimensionless perturbation wavenumber for $kh = 1$ and $X = -0.40$ (orange solid line), $X = 0$ (blue solid line), $X = 0.40$ (green solid line).

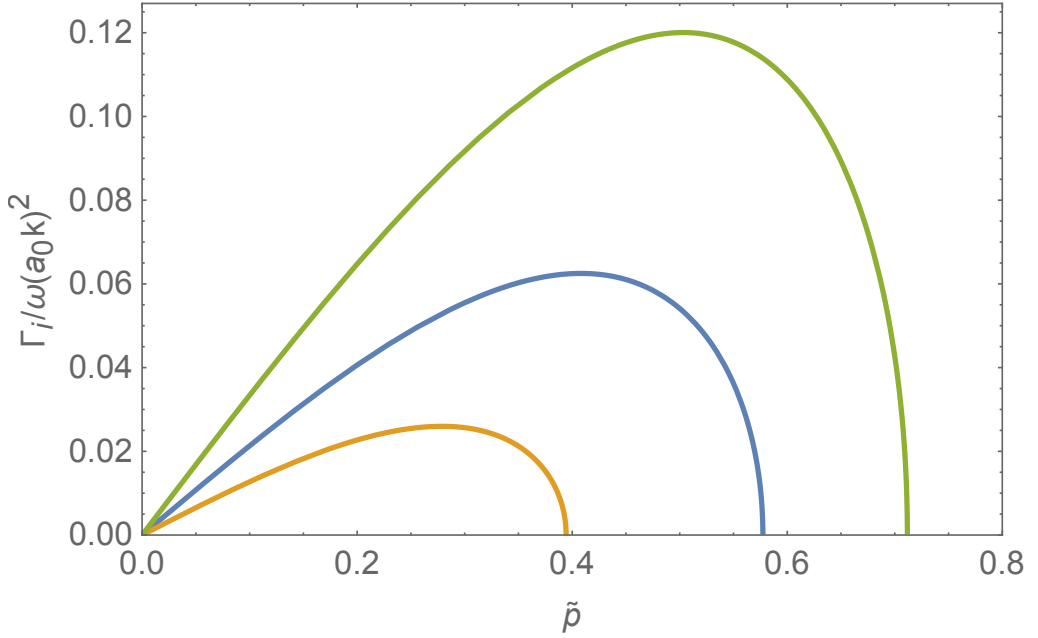


Figure 7: Dimensionless growth rate of instability as a function of the dimensionless perturbation wavenumber for $kh = \infty$ and $X = -0.40$ (orange solid line), $X = 0$ (blue solid line), $X = 0.40$ (green solid line)

290 rate as a function of the dimensionless wavenumber of the modulational perturbation for
 291 several values of the wave steepness of the carrier wave. The symbols correspond to the
 292 results of Tiron & Choi (2012) whereas the solid line corresponds to the results obtained
 293 with the vor-NLS equation. A quite good agreement between the two approaches is obtained
 294 when $a_0 k \leq 0.69$. Note that the maximal wave steepness of Crapper's capillary waves is
 295 $a_0 k \approx 2.29$.

296 The rate of decay of the amplitude of linear waves due to bulk viscosity is $2\nu k^2$ where ν is the
 297 kinematic viscosity and k the wavenumber. In the following we consider the modulational
 298 instability of capillary waves in the presence of dissipation due to viscosity and some forcing
 299 due for instance to wind. Note that this problem has been investigated by Kharif *et al.* (2010)
 300 for pure gravity waves in deep water. The latter authors used the Miles' mechanism to model
 301 wind effect.

302 Equation (2.6) becomes

$$303 \quad ia_\tau + La_{\xi\xi} + N|a|^2 a = i(\Delta - 2\nu k^2)a, \quad (3.9)$$

304 where $\Delta > 0$ corresponds to a forcing term.

305 Equation (3.9) admits the following solution,

$$306 \quad a_s = a_0 \exp(K\tau) \exp\left(\frac{iN}{2K} a_0^2 (e^{2K\tau} - 1)\right), \quad (3.10)$$

307 where $K = \Delta - 2\nu k^2$.

308 Note that a_s is spatially constant.

309 We superimpose to this solution a small disturbance

$$310 \quad a(\xi, \tau) = a_s (1 + \epsilon a'(\xi, \tau)), \quad (3.11)$$

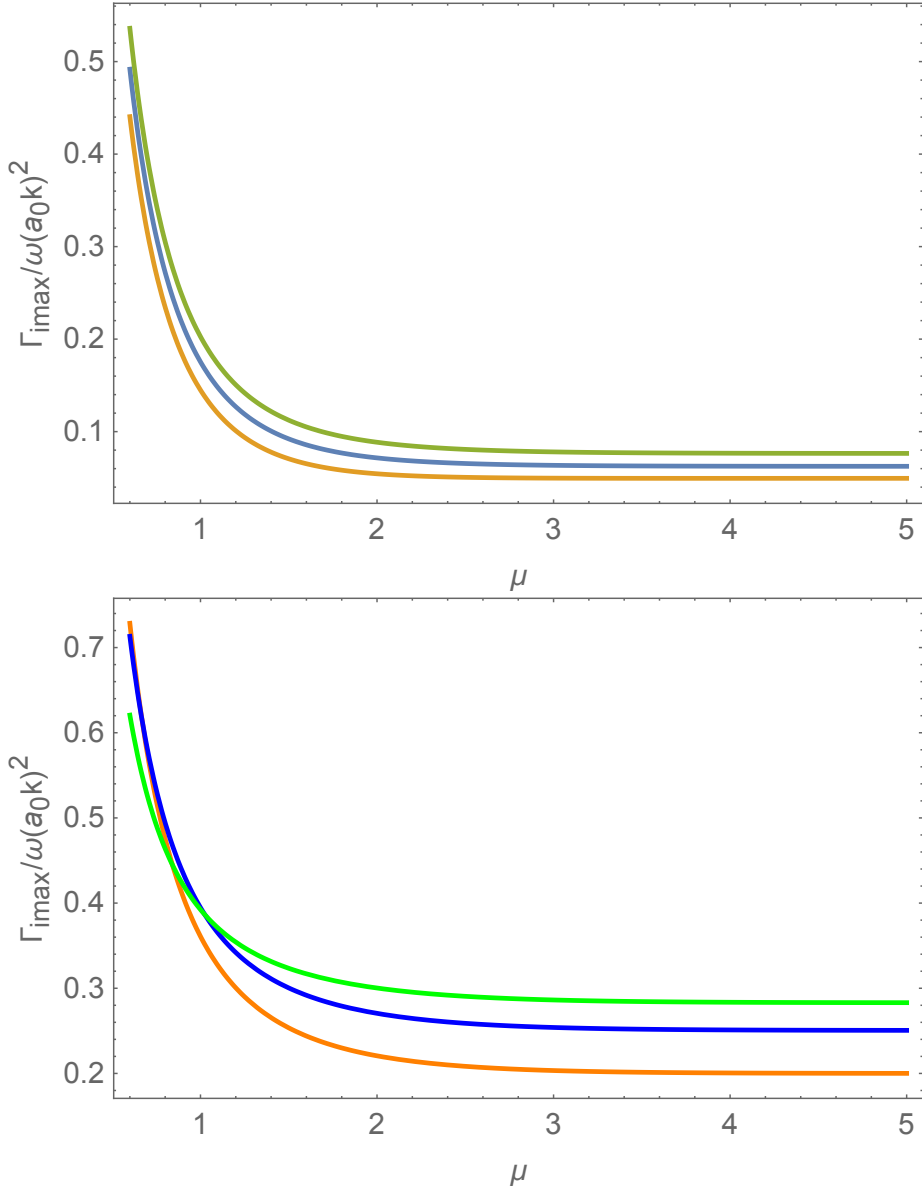


Figure 8: Dimensionless maximal growth rate of instability as a function of the dimensionless depth, $\mu = kh$. (Top) $X = -0.10$ (orange solid line), $X = 0$ (blue solid line), $X = 0.10$ (green solid line). (Bottom): $X = 1$ (orange solid line), $X = 1.5$ (blue solid line), $X = 2$ (green solid line)

311 with $\epsilon \ll 1$.

312 Substituting (3.11) into (3.9) and keeping only terms of order ϵ and separating the real and
 313 imaginary parts of $a'(\xi, \tau) = a'_r(\xi, \tau) + ia'_i(\xi, \tau)$ gives

$$314 \quad a'_{i\tau} - La'_{r\xi\xi} - 2Na_0^2 \exp(2K\tau)a'_r = 0.$$

315

$$316 \quad a'_{r\tau} + La'_{i\xi\xi} = 0.$$

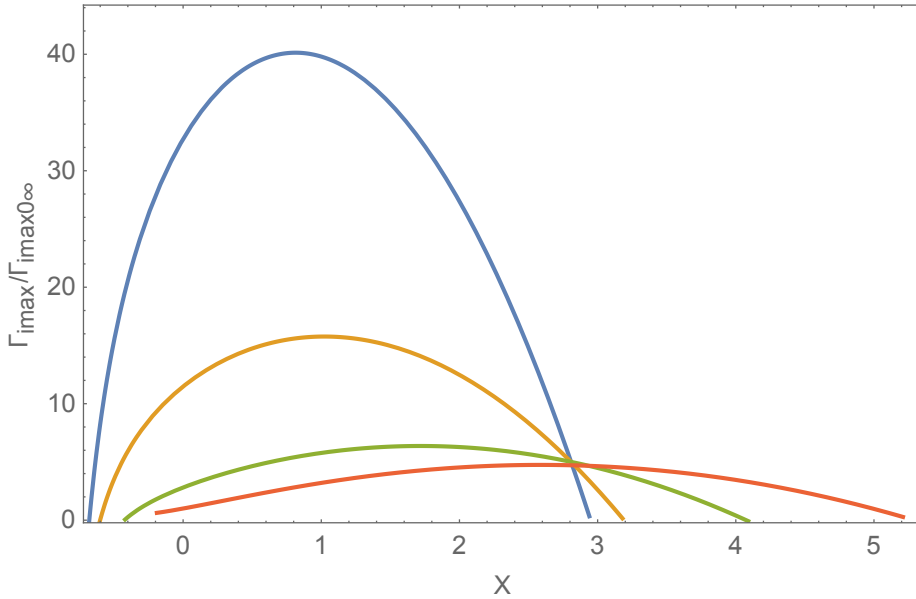


Figure 9: Dimensionless maximal growth rate of instability as a function of the vorticity for several dimensionless depths. $kh = 0.3$ (blue solid line), $kh = 0.5$ (orange solid line), $kh = 1$ (green solid line), $kh = \infty$ (red solid line). $\Gamma_{imax0\infty} = \Gamma_{imax}(\Omega = 0, kh = \infty)$.

317 Set $a'_r(\xi, \tau) = \text{Re}(a'_{r0}(\tau) \exp(ip\xi))$ and $a'_i(\xi, \tau) = \text{Im}(a'_{i0}(\tau) \exp(ip\xi))$ where p is the
 318 wavenumber of the perturbation. Then,

$$319 \quad \frac{da'_{i0}}{d\tau} + (Lp^2 - 2Na_0^2 \exp(2K\tau))a'_{r0} = 0.$$

320

$$321 \quad \frac{da'_{r0}}{d\tau} - Lp^2 a'_{i0} = 0.$$

322 Combining the two previous equations gives

$$323 \quad \frac{d^2 a'_{r0}}{d\tau^2} + L^2 p^4 \left(1 - \frac{2N}{Lp^2} a_0^2 \exp(2K\tau) \right) a'_{r0} = 0. \quad (3.12)$$

324 One may distinguish two cases according to whether K is negative or positive.

325 (i) Let K be negative. This case was analysed by Segur *et al.* (2005) and Kharif *et al.* (2010).
 326 In the presence of damping, the modulational instability is stabilised by viscous dissipation.
 327 However, note that the modulational instability may grow, but its growth is limited and
 328 starts to stabilise after a time $\tau = -\frac{1}{2K} \ln\left(\frac{2Na_0^2}{Lp^2}\right)$ corresponding to the change of sign of the
 329 coefficient of a'_{r0} of equation (3.12). Note that the bandwidth of instability shrinks as the
 330 amplitude of the carrier wave diminishes, resulting in stabilisation of unstable modes. The
 331 most unstable perturbation starts stabilisation at $\tau = \ln 2 / (4\nu k^2)$. Let us consider a carrier
 332 wave of wavelength $\lambda = 0.005 \text{ m}$ in deep water. For $X = 0$, stabilizing of the most unstable
 333 perturbation will start at $\tau \approx 7\tau_0$ where τ_0 is the dimensional period of the carrier wave. For
 334 $X = 0.4$ and $X = -0.4$, we found that the most unstable perturbation stabilises at $\tau \approx 6\tau_0$
 335 and $\tau \approx 9\tau_0$, respectively. These critical times are more or less confirmed by numerical
 336 simulations of dimensionless equation (3.14) (see figure 11) without forcing.

337 (ii) Let K be positive. This case was discussed by Kharif *et al.* (2010) who considered gravity

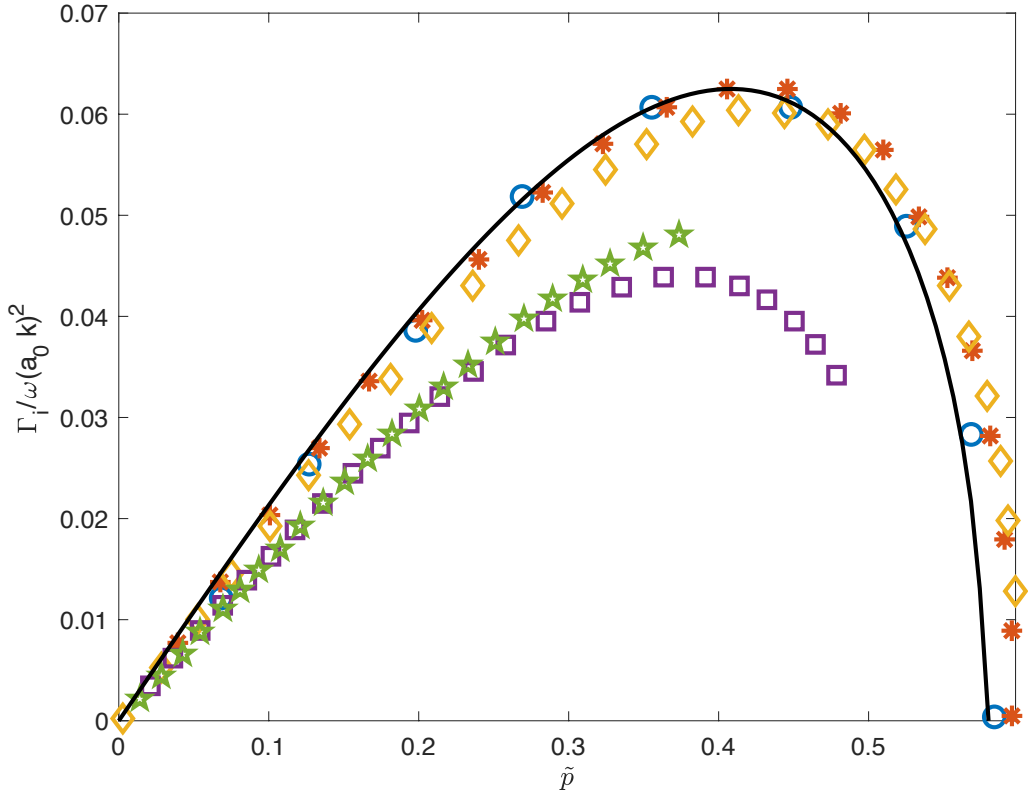


Figure 10: Dimensionless growth rate as a function of the dimensionless perturbation wavenumber in deep water with $X = 0$. Circles, $a_0 k = 0.25$; asterisk, $a_0 k = 0.47$; diamonds, $a_0 k = 0.69$; squares, $a_0 k = 1.03$; stars $a_0 k = 1.16$. The symbols correspond to the results of Tiron & Choi (2012) and the solid line corresponds to those of the vor-NLS equation.

338 wave trains on the surface of water acted upon by wind and under influence of viscosity.
 339 Herein, a similar situation is considered within the framework of pure capillary wave trains.
 340 In this case, the modulational perturbations are initially oscillating for $0 < \tau < \frac{1}{2K} \ln\left(\frac{2Na_0^2}{Lp^2}\right)$
 341 and then start to grow exponentially for $\tau > \frac{1}{2K} \ln\left(\frac{2Na_0^2}{Lp^2}\right)$. The bandwidth of instability
 342 increases as the amplitude of the carrier wave increases. Consequently, stable modes may
 343 become unstable. Let p be a perturbation wavenumber corresponding to a stable state. There
 344 is a critical value of the carrier wave amplitude, a_0 , for which the bandwidth instability
 345 is equal to p . For carrier wave amplitude larger than this critical value, the perturbation
 346 becomes unstable. The critical value is given by $\Gamma_i = 0$, that is to say,

$$347 \quad a_{0c}^2 = \frac{Lp^2}{2N} \quad (3.13)$$

348 The modulational instability will start to grow as soon as the carrier wave amplitude reaches
 349 the critical value. When the carrier wave amplitude is set equal to a_{0c} , the instability starts
 350 at $\tau = 0$.

351 Let us consider the case without vorticity ($X = 0$) in deep water. The dispersive and nonlinear
 352 coefficients of the vor-NLS equation are $L = 3\omega/(8k^2)$ and $\omega k^2/16$. The critical wave

353 steepness of the carrier wave is

$$354 \quad a_{0c}k = \sqrt{3} p/k$$

355 This critical value is more or less confirmed by numerical simulations of dimensionless
356 equation (3.14) (see figure 12-(a)) with forcing, $\tilde{K} = (\tilde{\Delta} - 2/R_e)$.

357 For $(X, p/k) = (0.4, 0.8)$ and $(X, p/k) = (-0.4, 0.5)$ we found, in deep water, $a_{0c}k \approx 1.12$
358 and 1.27, respectively (see figure 12-(b)-(c)).

359 To complete the linear stability analysis, we consider the nonlinear evolution of unstable and
360 stable modes. To do this, we use equation (3.9) written in dimensionless form with respect
361 to the reference length $1/k$ and reference time $1/\omega$ where k and ω are the wavenumber and
362 frequency of the carrier wave, respectively.

$$363 \quad i\tilde{a}_{\tilde{\tau}} + \tilde{L}\tilde{a}_{\tilde{\xi}\tilde{\xi}} + \tilde{N}|\tilde{a}|^2\tilde{a} = i(\tilde{\Delta} - \frac{2}{R_e})\tilde{a}, \quad (3.14)$$

364 where $R_e = \omega/(k^2\nu)$.

365 Within the framework of numerical simulations of the vor-NLS equation, figure 11 shows, in
366 the presence of viscous dissipation only and for several values of the vorticity, the temporal
367 evolution of the amplitude of the carrier wave, a_0 , and those of the most unstable sidebands,
368 a_{-1} and a_{+1} , whose curves overlap. At the beginning of the nonlinear interaction, the
369 modulational instability is growing due to a transfer of energy from the carrier wave to
370 the sidebands and then stabilises under the effect of the dissipation (see figure 11-(a)-(b)).
371 The case corresponding to figure 11-(c) presents a different behaviour because the initial rate
372 of growth of the instability and the rate of damping are of the same order, preventing the
373 instability from developing.

374 Figure 12 shows, in the presence of forcing, the temporal evolution of the amplitude of the
375 carrier wave, a_0 , and those of the initially stable sidebands, a_{-1} and a_{+1} for several values
376 of the vorticity. At the beginning, numerical simulations show that the perturbations are
377 oscillating and then are growing.

378 4. Capillary solitary waves on deep water in the presence of constant vorticity

379 Equation (2.6) admits as solution the envelope soliton given by the following expression

$$380 \quad a(\xi, \tau) = \pm a_0 \operatorname{sech}\left(a_0\left(\frac{N}{2L}\right)^{1/2}\xi\right) \exp(iNa_0^2\tau/2). \quad (4.1)$$

381 The corresponding surface elevation of a weakly nonlinear wave train of envelope given by
382 (4.1) is

$$383 \quad \zeta = \pm \frac{1}{2}\epsilon a_0 \operatorname{sech}\left(\sqrt{\frac{N}{2L}} a_0\epsilon(x - c_g t)\right) \exp\left(ikx - i(\omega - N\epsilon^2 a_0^2)t\right) + c.c., \quad (4.2)$$

384 where k and ω are the carrier wavenumber and carrier frequency and *c.c.* is the complex
385 conjugation.

386 Near the minimum of phase velocity of linear gravity-capillary waves, the phase velocity and
387 the group velocity are nearly equal. As stated by Longuet-Higgins (1993) in any dispersive
388 medium supporting envelope soliton and whose linear dispersion has an extremum we
389 can expect that steady solitary waves with decaying oscillatory tails bifurcate from linear
390 periodic waves. These waves are called generalized solitary waves to distinguish them from
391 those which are flat at $x = \pm\infty$. For a review on this problem, one can refer to Dias & Kharif
392 (1999). It is noteworthy to emphasize that pure periodic capillary wave train can bifurcate

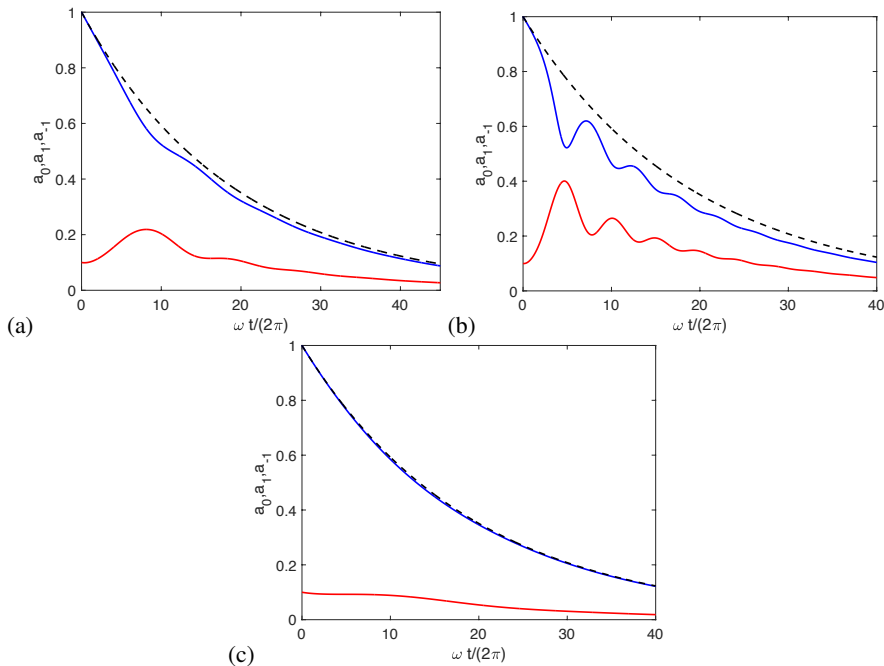


Figure 11: Temporal evolution of the dimensionless amplitudes of the carrier wave (solid blue line) and most unstable sideband modes (solid red line) in the presence of viscous dissipation in deep water. (a) $X = 0$, $R_e \approx 240$; (b) $X = 0.4$, $R_e \approx 202$; (c) $X = -0.4$, $R_e \approx 308$. Herein, $\omega = 1$.

393 into generalized solitary waves only in the presence of positive vorticity as mentioned in
 394 section 2. Bifurcation cannot occur for negative vorticity because there is no phase velocity
 395 minimum.

396 Following Akylas (1993) and Abid *et al.* (2019) we consider a train of periodic pure capillary
 397 waves on deep water bifurcating into a solitary wave with a decaying oscillatory tail in the
 398 presence of positive vorticity ($\Omega < 0$). Note that Akylas (1993) and Abid *et al.* (2019)
 399 considered gravity-capillary waves.

400 We use $T/(\rho_w c^2)$ and $T/(\rho_w c^3)$ as unit of length and unit of time, where c is the phase
 401 velocity of the envelope soliton. In this way c is the reference phase velocity scale. Note that
 402 this normalisation is equivalent to set $T = 1$, $\rho_w = 1$ and $c = 1$.

403 Within the framework of the new normalisation, the condition for the envelope soliton to be
 404 a solitary is

$$405 \quad \omega(k, \Omega) - \frac{1}{2} N a_0^2 \epsilon^2 = k, \quad \frac{\partial \omega}{\partial k} = 1. \quad (4.3)$$

406 Critical values of the parameters are obtained by setting $\epsilon = 0$ in (4.3)

$$407 \quad k_0 = \omega(k_0, \Omega_0), \quad \frac{\partial \omega}{\partial k}(k_0, \Omega_0) = 1. \quad (4.4)$$

408 Solving these two equations gives

$$409 \quad k_0 = \frac{1}{2}, \quad \Omega_0 = -\frac{1}{4}, \quad \omega_0 = \frac{1}{2} \quad (4.5)$$

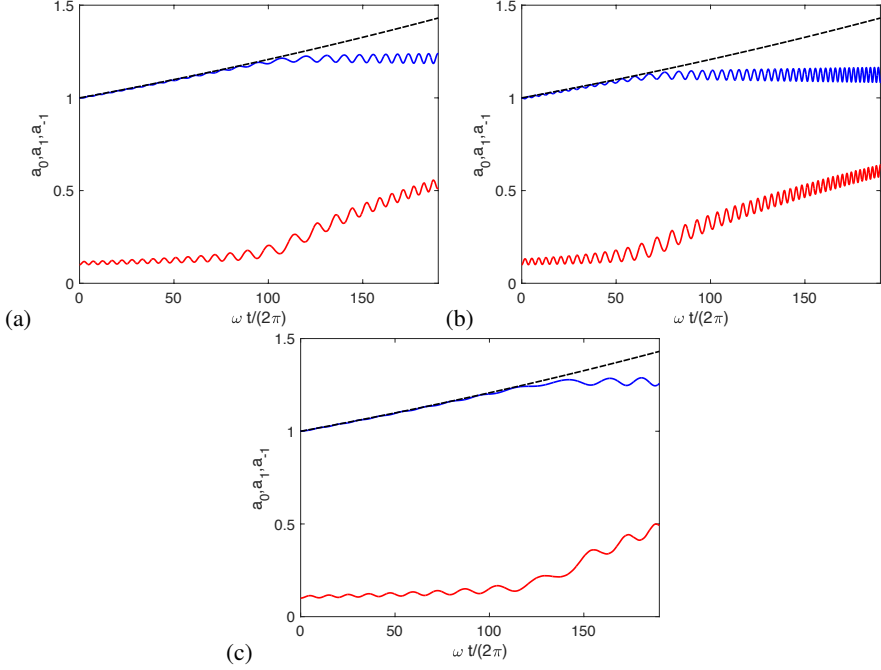


Figure 12: Temporal evolution of the dimensionless amplitudes of the carrier wave (solid blue line) and stable sideband modes (solid red line) in the presence of weak forcing in deep water. (a) $X = 0$, $p = 0.7$; (b) $X = 0.4$, $p = 0.8$; (c) $X = -0.4$, $p = 0.5$; $\tilde{K} = 3/10000$. Herein, $\omega = 1$.

410 The carrier wavenumber k and the shear Ω are expanded about (k_0, Ω_0) as follows

$$411 \quad k = k_0 + k_1 \epsilon^2 + \mathcal{O}(\epsilon^3).$$

412

$$413 \quad \Omega = \Omega_0 + \Omega_1 \epsilon^2 + \mathcal{O}(\epsilon^3).$$

414 Expanding $\omega(k, \Omega)$ about (k_0, Ω_0) and using

$$415 \quad k = \omega(k, \omega) - \frac{1}{2} N \epsilon^2 a_0^2,$$

416 with $\partial\omega/\partial k(k_0, \Omega_0) = 1$ gives

$$417 \quad \Omega_1 = \frac{1}{2} \frac{N(k_0, \Omega_0)}{\frac{\partial\omega}{\partial\Omega}(k_0, \Omega_0)} a_0^2.$$

418

$$419 \quad k_1 = -\frac{\frac{\partial^2\omega}{\partial k \partial\Omega}(k_0, \Omega_0)}{2L(k_0, \Omega_0)} \Omega_1. \quad (4.6)$$

420 Let $\delta\Omega$ be the difference between Ω and the critical value Ω_0

$$421 \quad \delta\Omega = \Omega_1 \epsilon^2 + \mathcal{O}(\epsilon^3).$$

422 The wave steepness of the generalized solitary wave is

$$423 \quad a_0^2 \epsilon^2 = 2 \frac{\frac{\partial\omega}{\partial\Omega}(k_0, \Omega_0)}{N(k_0, \Omega_0)} \delta\Omega, \quad (4.7)$$

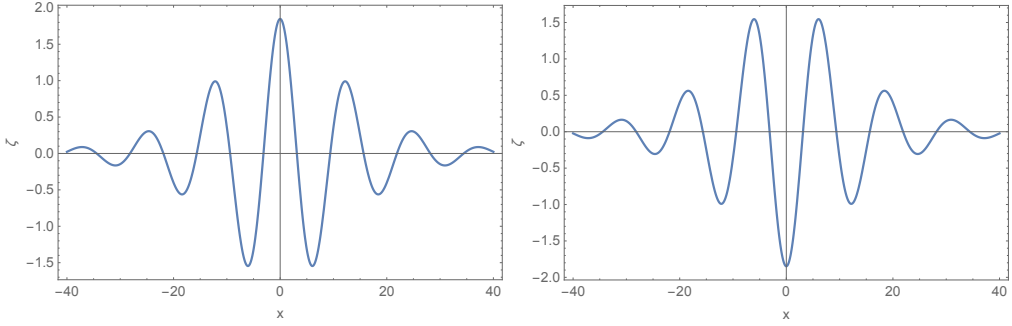


Figure 13: Dimensionless profiles of generalized capillary solitary waves of elevation (left) and depression (right) in deep water for $\delta\Omega = -0.01$

424 and

$$425 \quad k = k_0 - \frac{\partial^2 \omega}{\partial k \partial \Omega}(k_0, \Omega_0) \delta\Omega \quad (4.8)$$

426 Substituting the critical values given by (4.5) into (4.7) and (4.8) gives

$$427 \quad a_0^2 \epsilon^2 = -\frac{32^2}{3} \delta\Omega, \quad \delta\Omega < 0.$$

428

$$429 \quad k = k_0 - \frac{3}{16} \delta\Omega, \quad \delta\Omega < 0.$$

430 Consequently, the profile of the generalized solitary wave is

$$431 \quad \zeta(x, t) = \pm \frac{32}{\sqrt{3}} \sqrt{-\delta\Omega} \operatorname{sech}\left(\sqrt{-\delta\Omega}(x - t)\right) \cos\left(k(x - t)\right) \quad (4.9)$$

432 The profile of the generalized solitary wave is known once the bifurcation parameter $\delta\Omega$ is
 433 fixed. At $\Omega = \Omega_0$ the train of linear periodic capillary waves bifurcates into a solitary wave
 434 whose profile is given by (4.9). The (+) sign corresponds to a generalized solitary wave of
 435 elevation, whereas the (-) sign corresponds to a generalized solitary wave of depression.

436 The envelope soliton is unstable to transverse perturbations (see section 5). Consequently,
 437 capillary solitary waves with decaying oscillatory tails are expected to be unstable, too.

438 Within the framework of irrotational flow, Ifrim & Tataru (2020) proved rigorously that there
 439 are no capillary solitary waves in deep water with a free surface asymptotically flat at infinity.
 440 We have shown that capillary solitary waves with decaying oscillatory tails in the presence of
 441 constant positive vorticity may exist in deep water. Within the framework of rotational flows,
 442 we have shown that generalized capillary solitary waves may exist. In figures 13 and 14 are
 443 plotted the dimensionless profiles of generalized capillary solitary waves in deep water for
 444 two values of the bifurcation parameter $\delta\Omega$. The profiles become flatter when $|\delta\Omega|$ increases.
 445 This feature could suggest the existence of capillary solitary waves being flat in the far-field
 446 at the free surface of rotational flows of positive vorticity in deep water.

447 5. Transverse instability of the capillary envelope soliton and capillary Stokes 448 wave in deep water with constant vorticity

449 In the two following subsections, we consider the stability of the capillary envelope soliton and
 450 capillary Stokes waves to transverse perturbations. Note that the vorticity of the underlying
 451 current is now perturbed by the infinitesimal periodic vorticity due to the perturbation, while

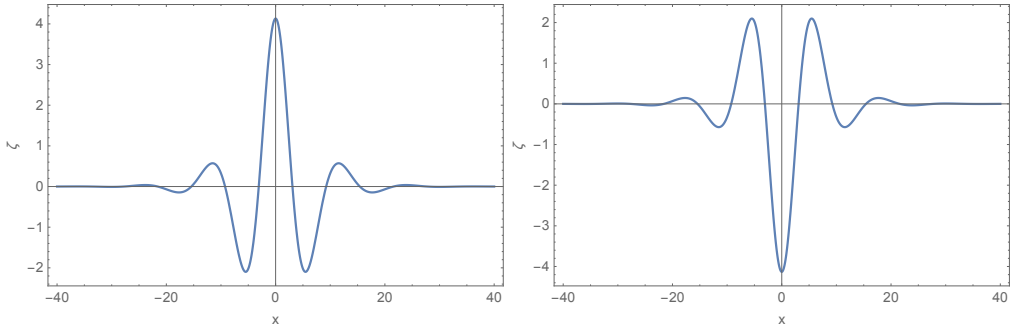


Figure 14: Dimensionless profiles of generalized capillary solitary waves of elevation (left) and depression (right) in deep water for $\delta\Omega = -0.05$

452 in $1D$ propagation the perturbation is potential and does not affect the shear. Nevertheless,
 453 the phase average of the vorticity is $-\Omega$.

5.1. Capillary envelope soliton

455 In $2D$ the NLS equation in deep water reads

$$456 \quad ia_\tau + La_{\xi\xi} + Ma_{\eta\eta} + N|a|^2a = 0, \quad (5.1)$$

457 with

$$458 \quad L = \frac{3\omega}{k^2} \left(\frac{(1+X)(1+X+X^2)}{(2+X)^3} \right),$$

$$460 \quad N = \frac{\omega k^2}{24} \left(\frac{3+14X+23X^2+11X^3-3X^4}{(X+1)(3X+2)} \right),$$

$$462 \quad M = \frac{3T}{2\rho_w} \left(\frac{k}{\omega(2+X)} \right).$$

463 Herein $X = \Omega/\omega$.

464 Equation (5.1) admits as solution the two-dimensional envelope soliton, $\bar{a}(\xi, \tau)$, given by
 465 (4.1). We consider the stability of this solution to infinitesimal disturbances

$$466 \quad a(\xi, \eta, \tau) = \bar{a}(\xi, \tau) + a'(\xi, \eta, \tau) \exp\left(iNa_0^2\tau/2\right). \quad (5.2)$$

467 The stability analysis is similar to that used by Abid *et al.* (2019) for gravity-capillary
 468 envelope soliton, except that now the coefficients of the NLS equation correspond to pure
 469 capillary envelope soliton. Linearisation of (5.1) about \bar{a} with $a' = u + iv$ gives

$$470 \quad v_\tau = Lu_{\xi\xi} + Mu_{\eta\eta} + (3NA^2 - Na_0^2/2)u, \quad (5.3)$$

$$472 \quad u_\tau = -Lv_{\xi\xi} - Mv_{\eta\eta} - (NA^2 - Na_0^2/2)v, \quad (5.4)$$

473 where

$$474 \quad A = a_0 \operatorname{sech}\left(a_0 \left(\frac{N}{2L}\right)^{1/2} \xi\right)$$

475 The system (5.3)-(5.4) of linear partial differential equations with constant coefficients admits
 476 solutions of the following form

$$477 \quad u = \hat{u}(\xi) \exp(iq\eta + \Gamma\tau), \quad (5.5)$$

478

$$v = \hat{v}(\xi) \exp(iq\eta + \Gamma\tau). \quad (5.6)$$

479

480 Substitution of (5.5) and (5.6) into (5.3) and (5.4) gives

481

$$\Gamma\hat{v} = L\frac{d^2\hat{u}}{d\xi^2} - Mq^2\hat{u} + (3NA^2 - Na_0^2/2)\hat{u}, \quad (5.7)$$

482

483

$$\Gamma\hat{u} = -L\frac{d^2\hat{v}}{d\xi^2} + Mq^2\hat{v} - (NA^2 - Na_0^2/2)\hat{v}. \quad (5.8)$$

484 The eigenfunction \hat{v} can be eliminated

485

$$\Gamma^2\hat{u} = -(D_0 - Mq^2)(D_1 - Mq^2)\hat{u}, \quad (5.9)$$

486 with

487

$$D_0 = L\frac{d^2}{d\xi^2} + NA^2 - Na_0^2/2,$$

488

489

$$D_1 = L\frac{d^2}{d\xi^2} + 3NA^2 - Na_0^2/2.$$

490 The eigenfunction $\hat{u} \rightarrow 0$ as $\xi \rightarrow \infty$ (the eigenfunctions are local in ξ). Note that the
 491 non-local states corresponding to the continuum spectrum are stable or marginally stable
 492 (Saffman & Yuen (1978) and Rypdal & Rasmussen (1989)).

493 The numerical method used to solve (5.9) is outlined in Appendix A of Abid *et al.* (2019).

494 Without loss of generality, we set $T = 1$, $\rho_w = 1$ and $k = 1$ as Saffman & Yuen (1985)
 495 and Tiron & Choi (2012). For the sake of clarity, the same symbols are used to call the
 496 coefficients of the NLS equation. For comparison, we consider the analytic expression of the
 497 instability growth rate derived by Rypdal & Rasmussen (1989) and Abid *et al.* (2019), given
 498 in dimensionless form by

499

$$\Gamma^2 = \frac{32}{\pi^2}MNq^2\left(1 - \frac{M}{3N}q^2\right). \quad (5.10)$$

500

501

$$\Gamma_{max}^2 = \frac{24}{\pi^2}N^2,$$

502 with

503

$$q_{max} = \sqrt{\frac{3N}{2M}}.$$

504 The capillary envelope soliton is unstable to infinitesimal transverse perturbations of
 505 wavenumber q satisfying $q^2 < 3N/M$. Figure 15 shows the square of the dimensionless
 506 growth rate as a function of the square of the dimensionless transverse wavenumber for
 507 different values of the vorticity. The numerical and analytic results are in excellent agreement.
 508 The dimensionless growth rate and instability bandwidth increase as the dimensionless
 509 vorticity decreases. Note that in deep water

510

$$\Omega^2 = \frac{Tk^3}{\rho_w} \frac{X^2}{1+X} \quad \text{with} \quad X > -1,$$

511 and in dimensionless form

512

$$\Omega^2 = \frac{X^2}{1+X}.$$

513

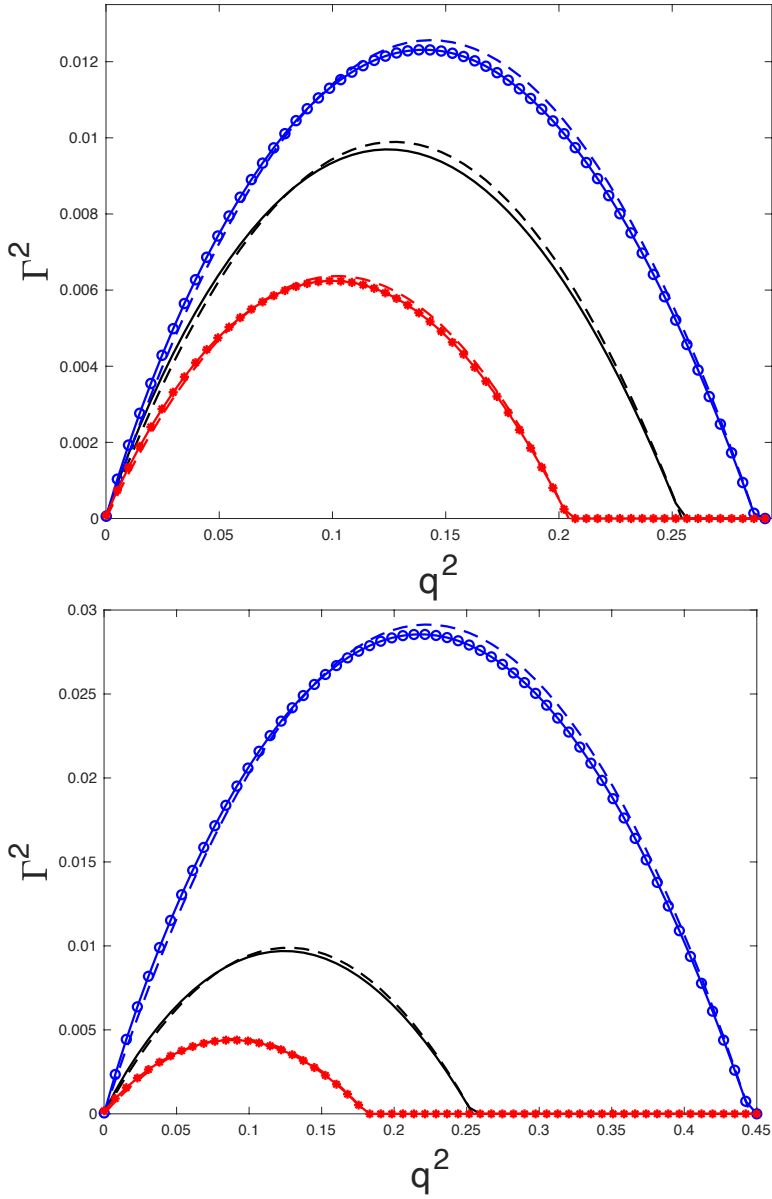


Figure 15: Square of the dimensionless growth rate of the transverse unstable mode of capillary envelope soliton in deep water as a function of the square of the dimensionless wavenumber for (top) $X = -0.1$ (*), $X = 0$ (solid line), $X = 0.1$ (o) and (bottom) $X = -0.5$ (*), $X = 0$ (solid line), $X = 0.5$ (o). The dashed lines correspond to the analytic expression given by (5.10).

514

5.2. Capillary Stokes waves

515 Equation (5.1) admits as solution the Stokes wave envelope given by (3.1). This solution is
 516 unstable to perturbations of longitudinal and transverse wavenumbers p and q if

517

$$Lp^2 + Mq^2 < 2Na_0^2. \quad (5.11)$$

518 Using the linear dispersion (2.9) the coefficient M is rewritten as follows

$$519 \quad M = \frac{3\omega}{2k^2} \frac{1+X}{2+X}$$

520 In a more explicit form, condition (5.11) reads

$$521 \quad \frac{3(1+X)(1+X+X^2)}{(2+X)^3} p^2 + \frac{3(1+X)}{2(2+X)} q^2 < \frac{3+14X+23X^2+11X^3-3X^4}{12(1+X)(2+3X)} a_0^2 k^4 \quad (5.12)$$

522 The instability condition $p^2 + 2q^2 < k^4 a_0^2 / 3$, established by Chen & Saffman (1985), is
523 recovered for $X = 0$.

524 The square of growth rate of instability is

$$525 \quad \Gamma_i^2 = (Lp^2 + Mq^2)(2Na_0^2 - Lp^2 - Mq^2) \quad (5.13)$$

526 Substituting the expressions of L , M and N into (5.13), we obtain in dimensionless form

$$527 \quad \frac{\Gamma_i^2}{\omega^2} = \frac{3(1+X)}{2+X} \left(\frac{1+X+X^2}{(2+X)^2} \frac{p^2}{k^2} + \frac{q^2}{2k^2} \right) \left(\frac{3+14X+23X^2+11X^3-3X^4}{12(1+X)(2+3X)} a_0^2 k^2 \right. \\ 528 \quad \left. - \frac{3(1+X)}{2+X} \left(\frac{1+X+X^2}{(2+X)^2} \frac{p^2}{k^2} + \frac{q^2}{2k^2} \right) \right) \quad (5.14)$$

530 For $X = 0$ we recover the growth rate of instability of Chen & Saffman (1985) given by

$$531 \quad \Gamma_i = \frac{1}{8} (3a_0^2 k^3 (p^2 + 2q^2) - \frac{9}{k} (p^2 + 2q^2)^2)^{1/2}. \quad (5.15)$$

532 Note that Chen & Saffman (1985) used the relation $\omega^2 = k^3$.

533 The boundary of the stability diagram in the $(p/k, q/k)$ -plane is given by the following
534 ellipse equation

$$535 \quad \frac{(1+X+X^2)}{(2+X)^2} \left(\frac{p}{k} \right)^2 + \frac{1}{2} \left(\frac{q}{k} \right)^2 = \frac{3+14X+23X^2+11X^3-3X^4}{36(1+X)^2} a_0^2 k^2. \quad (5.16)$$

536 Figure 16 shows the stability diagram in the $(p/k, q/k)$ -plane for three values of the
537 dimensionless vorticity. The domain of instability increases as the vorticity decreases. Dots
538 plotted in the figure, located on the p -axis, corresponds to the dimensionless maximal
539 growth rate of modulational instability. Consequently, the dominant modulational instability
540 of weakly nonlinear capillary waves on deep water is two-dimensional. The wavelength of
541 the dominant modulational instability increases as the vorticity decreases. For $\Omega = 0$ we
542 found $p/k = 0.0416$ which is very close to the value obtained by chen & Saffman (1985) in
543 their Table 1.

544 6. Conclusion

545 A nonlinear Schrödinger equation for pure capillary waves on arbitrary depth with a shear
546 current of constant vorticity has been derived, which completes the previous works of Thomas
547 *et al.* (2012) and Hsu *et al.* (2018) on gravity waves and gravity-capillary waves, respectively.
548 We have shown that the Wilton ripple phenomenon exists in infinite depth for pure capillary
549 waves propagating on a current of constant positive vorticity and that the second singularity of
550 the nonlinear coefficient of the vor-NLS equation corresponds to resonant triads of capillary
551 waves in finite depth with positive vorticity.

552 The influence of the vorticity on the modulational instability of weakly nonlinear capillary

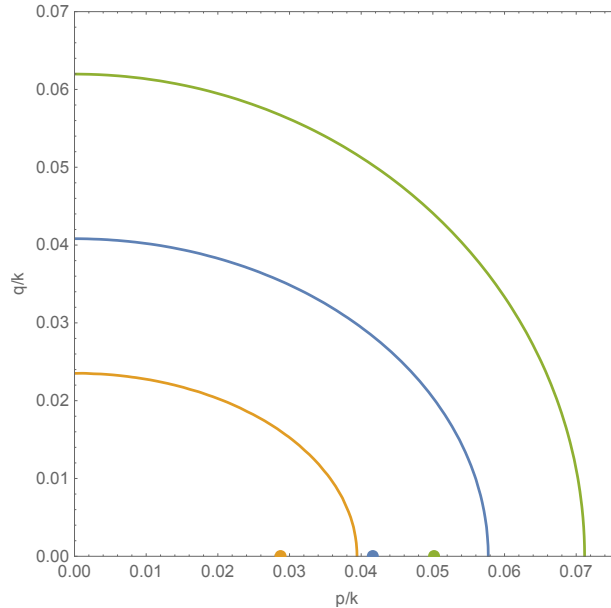


Figure 16: Stability diagram in the $(p/k, q/k)$ -plane for $a_0 k = 0.1$ and three values of the vorticity. Blue: $\Omega = 0$. Orange: $\Omega = -0.4$. Green: $\Omega = 0.4$. Dots correspond to the maximal growth rate of instability.

553 waves on arbitrary depth has been investigated in detail. We found that the dimensionless
 554 growth rate of modulational instability increases as the dimensionless vorticity decreases
 555 whatever the dispersive parameter, kh , where k is the carrier wavenumber and h the depth.
 556 The dimensionless maximal growth rate is strongly amplified for shallow water depths. The
 557 dimensionless bandwidth of instability increases as the dimensionless vorticity decreases.
 558 To measure the effect of bulk viscosity on the modulational instability of pure capillary
 559 waves travelling on a current of constant vorticity, we have considered the damped vor-
 560 NLS equation. The linear stability analysis reduces to a Sturm-Liouville problem. We
 561 found that the most unstable perturbation stabilizes faster for negative vorticity and later
 562 for positive vorticity. This was confirmed by numerical simulations of the damped vor-NLS
 563 equation in deep water. In the presence of a forcing term, we have used the forced vor-NLS
 564 equation. We found that a stable perturbation will become unstable as soon as the carrier
 565 wave amplitude reaches a critical value, which depends on the vorticity and the wavenumber
 566 of the perturbation. Furthermore, a stability analysis of weakly nonlinear capillary waves in
 567 deep water to transverse perturbations, has shown that the dominant modulational instability
 568 is two-dimensional whatever the vorticity.
 569 Within the framework of rotational flows of positive vorticity, we have shown, near the
 570 minimum of phase velocity of linear capillary waves on deep water, that generalized capillary
 571 solitary waves bifurcate from linear periodic capillary waves.
 572 We investigated the linear stability of the envelope soliton of pure capillary waves to transverse
 573 perturbation in deep water. We found that the dimensionless growth rate and instability
 574 bandwidth increase as the dimensionless vorticity decreases.

REFERENCES

- 575 ABID, M., KHARIF, C., HSU, H.-C. & CHEN, Y.-Y. 2019 Transverse instability of gravity–capillary solitary
 576 waves on deep water in the presence of constant vorticity. *Journal of Fluid Mechanics* **871**, 1028–
 577 1043.
- 578 AKYLAS, T. R. 1993 Envelope solitons with stationary crests. *Physics of Fluids A: Fluid Dynamics* **5** (4),
 579 789–791, arXiv: https://pubs.aip.org/aip/pof/article-pdf/5/4/789/12665842/789_1_online.pdf.
- 580 CHEN, B. & SAFFMAN, P. G. 1985 Three-dimensional stability and bifurcation of capillary and gravity waves
 581 on deep water. *Studies in Applied Mathematics* **72**, 125–147.
- 582 CONSTANTIN, A. & KARTASHOVA, E. 2009 Effect of non-zero constant vorticity on the nonlinear resonances
 583 of capillary water waves. *EPL (Europhysics Letters)* **86** (2), 29001.
- 584 CRAPPER, G. D. 1957 An exact solution for progressive capillary waves of arbitrary amplitude. *Journal of*
 585 *Fluid Mechanics* **2** (6), 532–540.
- 586 DHAR, A. K. & KIRBY, JAMES T. 2023 Fourth-order stability analysis for capillary-gravity waves
 587 on finite-depth currents with constant vorticity. *Physics of Fluids* **35** (2), 026601, arXiv:
 588 https://pubs.aip.org/aip/pof/article-pdf/doi/10.1063/5.0136002/16681631/026601_1_online.pdf.
- 589 DIAS, FRÉDÉRIC & KHARIF, CHRISTIAN 1999 Nonlinear gravity and capillary-gravity waves. *Annual Review*
 590 *of Fluid Mechanics* **31** (1), 301–346.
- 591 DJORDJEVIC, V DJ & REDEKOPP, LARRY G 1977 On two-dimensional packets of capillary-gravity waves.
 592 *Journal of Fluid Mechanics* **79** (4), 703–714.
- 593 HOGAN, SJ 1985 The fourth-order evolution equation for deep-water gravity-capillary waves. *Proceedings*
 594 *of the Royal Society of London. A. Mathematical and Physical Sciences* **402** (1823), 359–372.
- 595 HOGAN, SJ 1988 The superharmonic normal mode instabilities of nonlinear deep-water capillary waves.
 596 *Journal of Fluid Mechanics* **190**, 165–177.
- 597 HSU, H. C., KHARIF, C., ABID, M. & CHEN, Y. Y. 2018 A nonlinear schrödinger equation for gravity-
 598 capillary water waves on arbitrary depth with constant vorticity. part 1. *Journal of Fluid Mechanics*
 599 **854**, 146–163.
- 600 IFRIM, MIHAELA & TATARU, DANIEL 2020 No solitary waves in 2d gravity and capillary waves in deep water.
 601 *Nonlinearity* **33** (10).
- 602 KHARIF, C., KRAENKEL, R. A., MANNA, M. A. & THOMAS, R. 2010 The modulational instability in deep
 603 water under the action of wind and dissipation. *Journal of Fluid Mechanics* **664**, 138–149.
- 604 KIM, BOGUK & AKYLAS, TR 2005 On gravity–capillary lumps. *Journal of Fluid Mechanics* **540**, 337–351.
- 605 LONGUET-HIGGINS, MICHAEL S 1989 Capillary–gravity waves of solitary type on deep water. *Journal of*
 606 *Fluid Mechanics* **200**, 451–470.
- 607 LONGUET-HIGGINS, MICHAEL S 1993 Capillary–gravity waves of solitary type and envelope solitons on deep
 608 water. *Journal of Fluid Mechanics* **252**, 703–711.
- 609 MARTIN, CALIN IULIAN & MATIOC, BOGDAN-VASILE 2013 Existence of Wilton Ripples for Water Waves with
 610 Constant Vorticity and Capillary Effects. *SIAM Journal on Applied Mathematics* **73** (4), 1582–1595.
- 611 MCLEAN, JOHN W. 1982 Instabilities of finite-amplitude water waves. *Journal of Fluid Mechanics* **114** (-1),
 612 315.
- 613 MILEWSKI, PAUL A 2005 Three-dimensional localized solitary gravity-capillary waves .
- 614 MURASHIGE, SUNAO & CHOI, WOORYOUNG 2020 Linear stability of transversely modulated finite-amplitude
 615 capillary waves on deep water. *Studies in Applied Mathematics* **146** (2), 498–525.
- 616 PĂRĂU, EI, VANDEN-BROECK, J-M & COOKER, MJ 2005 Nonlinear three-dimensional gravity–capillary
 617 solitary waves. *Journal of Fluid Mechanics* **536**, 99–105.
- 618 RYPDAL, K & RASMUSSEN, J JUUL 1989 Stability of solitary structures in the nonlinear schrödinger equation.
 619 *Physica Scripta* **40** (2), 192.
- 620 SAFFMAN, PG & YUEN, HC 1985 Three-dimensional waves on deep water. *Advances in nonlinear waves* .
- 621 SAFFMAN, PG & YUEN, HENRY C 1978 Stability of a plane soliton to infinitesimal two-dimensional
 622 perturbations. *The Physics of Fluids* **21** (8), 1450–1451.
- 623 SEGUR, H., HENDERSON, D. & CARTER, J. 2005 Stabilizing the benjamin–feir instability. *Journal of Fluid*
 624 *Mechanics* **539**, 229–271.
- 625 THOMAS, R., KHARIF, C. & MANNA, M. 2012 A nonlinear Schrödinger equation for water waves on finite
 626 depth with constant vorticity. *Physics of Fluids* **24** (12), 127102.
- 627 TIRON, ROXANA & CHOI, WOORYOUNG 2012 Linear stability of finite-amplitude capillary waves on water of
 628 infinite depth. *Journal of Fluid Mechanics* **696**, 402–422.

629 ZHANG, JUN & MELVILLE, W. K. 1986 On the stability of weakly-nonlinear gravity-capillary waves. *Wave*
630 *Motion* **8**, 439–454.

631 **Supplementary data.** No supplementary data.

632 **Acknowledgements.**

633 **Funding.** This research received no specific grant from any funding agency, commercial or not-for-profit
634 sectors.

635 **Declaration of interests.** The authors report no conflict of interest.

636 **Data availability statement.** The data that support the findings of this study are available upon request.

637 **Author ORCIDs.** C. Kharif, <https://orcid.org/0000-0003-0716-8183>; M. Abid, [https://orcid.org/0000-0002-](https://orcid.org/0000-0002-0438-4182)
638 0438-4182

639 **Author contributions.** Christian Kharif: Formal analysis; Investigation; Project administration; Method-
640 ology; Validation; Writing. Malek Abid: Formal analysis; Investigation; Project administration; Software;
641 Validation; Visualization; Writing; Data curation. Yang-Yih Chen: Formal analysis; Project administration.
642 Hung-Chu Hsu: Formal analysis; Project administration.